

Damage modelling of composites: validation of an interlaminar damage model at the element level in an industrial application

In this paper, the LMS Samtech Samcef finite element code is used to assess the damage tolerance of composite structures. Delamination (ply separation), which is one of the most dangerous and predominant failure modes in laminated composites, is addressed. Two methods are used. The first one is based on a pure fracture mechanics approach, namely VCE (virtual crack extension), while the second method relies on cohesive elements and on continuum damage mechanics. These methods are implemented in the commercial version of LMS Samtech Samcef. This means that, besides the commercial FE solver, no additional (and costly) plug-ins providing such capabilities are required to solve the problem. Another advantage is that the user does not have to implement academic methods or models that may be described in the literature. Even if the openness of LMS Samtech Samcef is available via material user routines, a native implementation in a commercial software program always provides a more reliable solution.

Figure 1 illustrates the damage in a laminated structure resulting from an impact at different energy levels. When the impact energy is low, that is for a quasi-static loading, flaws (and especially delaminations) appear inside the part but this damage is invisible (or barely visible) from the outside. Although the user is not aware of it, initial damage is present in the structure. As such an initial damage will penalize the mechanical performance of the composite material, it must be taken into account in the design of the part. This situation is studied here.

In this paper, the authors assess the dangerousness of initial interlaminar cracks and predict the non-linear mechanical response and the propagation of delamination in a composite part submitted to a quasi-static loading and including initial defects.

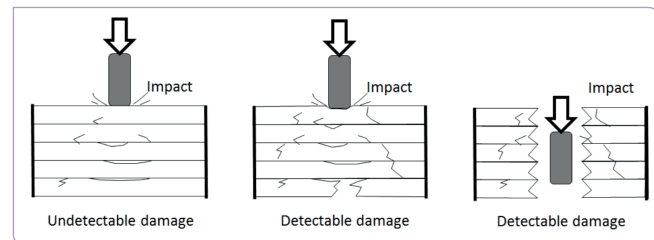
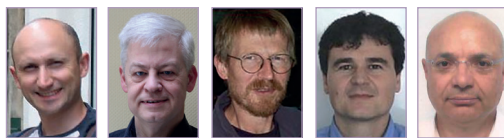


Fig. 1: Flaws in an impacted laminated composite structure

Here, we concentrate on the element level of the pyramid of tests illustrated in Figure 2. Additional validations of the LMS Samtech Samcef damage laws for damage tolerance of composites at the coupon and component levels can be found in [1-4].

By



Michael Bruyneel, R&D Team Manager (1) & Lecturer (2),
 Jean-Pierre Delsemme, Product Manager (1),
 Philippe Jetteur, Scientific Advisor (1),
 Fabrice Germain, Team leader, Engineering Services (1),
 Nourrédine Boudjemaa, Composite Material Stress Analysis Expert (3)
 (1) SAMTECH s.a.
 (2) Aerospace and Mechanical Engineering Department,
 University of Liège
 (3) LATECOERE

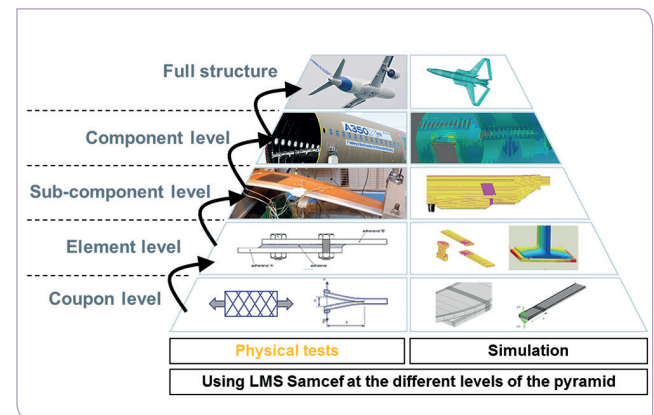


Fig. 2: Building block approach including the composite structure and virtual and experimental material testing. With courtesy of Airbus Innovations Works.

The VCE method

In this fracture mechanics approach, which is very similar to VCCT (virtual crack closure technique), the energy release rates by mode G_I , G_{II} and G_{III} (opening, shearing and tearing modes, respectively, see Figure 3) are computed at each node modelling the crack fronts, as illustrated in Figure 4.

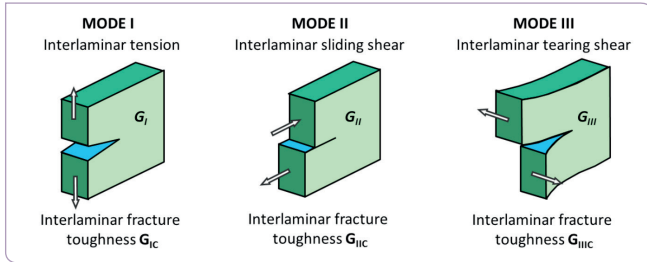


Fig. 3: The 3 modes of a crack propagation

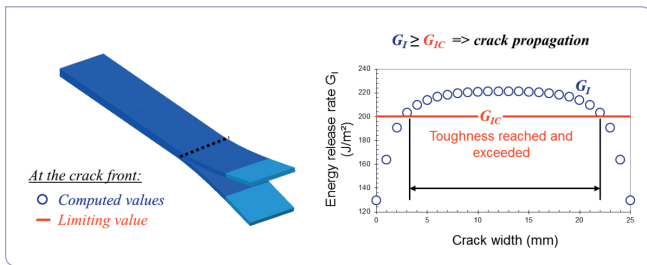


Fig. 4: Computation of the energy release rate at the nodes modelling the crack front

First, the total energy release rate is given by a finite difference on the potential energy π with respect to a local virtual crack propagation ΔA , where π_{init} and π_{pert} correspond to the energy associated to the initial and perturbed crack size, respectively:

$$G_T = -\frac{\Delta\pi}{\Delta A} = -\frac{\pi_{pert} - \pi_{init}}{\Delta A} = G_I + G_{II} + G_{III}$$

Then the contributions to the different modes are evaluated based on G_T and on the relative displacements U_i and reaction forces R_i in the local coordinate system attached to each node modelling the crack front:

$$G_I = \left(U_1 R_1 / \sum_{i=1}^3 U_i R_i \right) G_T \quad G_{II} = \left(U_2 R_2 / \sum_{i=1}^3 U_i R_i \right) G_T \quad G_{III} = \left(U_3 R_3 / \sum_{i=1}^3 U_i R_i \right) G_T$$

Once computed, these values are inserted in a failure criterion, for instance (1), in order to check whether or not the crack will propagate:

$$\frac{G_I}{G_{Ic}} + \frac{G_{II}}{G_{IIc}} + \frac{G_{III}}{G_{IIIc}} < 1? \quad (1)$$

In (1), G_{Ic} , G_{IIc} and G_{IIIc} are the fracture toughness values, which are determined based on specific (sometimes standardized) tests such as DCB (double cantilever beam) and ENF (end notched flexure). See [5] for more details.

In LMS Samtech Samcef, VCE is not used to simulate the crack propagation, mainly for two reasons. The first one is that VCE (just like VCCT) is a fracture mechanics approach. It is well known, and this is demonstrated even on simple configurations (see e.g. [5,6]), that a very fine mesh is needed in the vicinity of the crack front to obtain accurate results. The second reason is linked to the simulation of the crack propagation itself. In order to keep a model with a reasonable size, the mesh refinement should follow the crack front during propagation. For composites, re-meshing is a difficult task, because the crack fronts don't remain straight during propagation and only hexahedral (or prismatic) solid elements can be used when 3D laminates are modelled [7]. Moreover, the strategy for the crack propagation itself is either based on a geometric parameterization – which is very difficult to implement when several cracks must be managed – or based on nodes release [8]. In both cases, a general and robust solution procedure is difficult to implement and only simple cracked configurations have been successfully studied.

The cohesive elements approach

In the cohesive elements approach, zero thickness interface elements are defined between the hexahedral elements representing the plies (Figure 5).

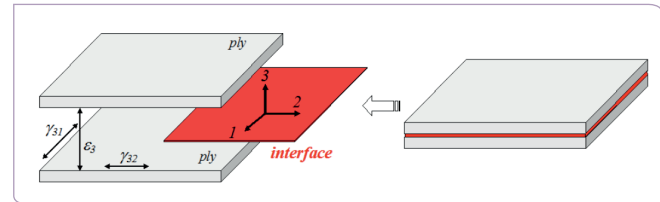


Fig. 5: Interface element

A specific material model including damage is assigned to these interface elements. In LMS Samtech Samcef, the approach described in [9] is implemented and extended in [10,5] in order to propose exponential, bi-triangular and polynomial constitutive laws for the interface (Figure 6). A potential e_d including the damage variables d_I , d_{II} and d_{III} is defined in order to represent the 3 modes of crack propagation of Figure 3. Only the components of the strain tensor relevant in the interface are considered (ϵ_{33} , γ_{31} and γ_{32}). As usual in continuum damage mechanics, the damage d_i impacts the initial material stiffness, here noted k_i^0 . The damage does not appear when the crack tends to be closed, that is for $\langle \epsilon_{33} \rangle_-$.

$$e_d = \frac{1}{2} \left[k_I^0 \langle \epsilon_{33} \rangle_-^2 + k_I^0 (1 - d_I) \langle \epsilon_{33} \rangle_+^2 + k_{II}^0 (1 - d_{II}) \gamma_{31}^2 + k_{III}^0 (1 - d_{III}) \gamma_{32}^2 \right]$$

The damage variables take their values between 0 (initial value; no damage) and 1 (final value; completely damaged interface). The value of the damage increases with the loading, which is associated to the so-called thermodynamic forces. In order to manage mixed mode behaviours, an equivalent thermodynamic

force Y is defined based on the pure contributions Y_I , Y_{II} and Y_{III} in order to represent the global effect of the loading:

$$Y = \sup_{\tau \leq t} G_{IC} \left\{ \left(\frac{Y_I}{G_{IC}} \right)^\alpha + \left(\frac{Y_{II}}{G_{IIC}} \right)^\alpha + \left(\frac{Y_{III}}{G_{IIIC}} \right)^\alpha \right\}^{1/\alpha}$$

Here, α is equal to 1. In [9], a single damage variable d is used to represent the damage, assuming that damage is damage, whatever may be the influencing mode. Details can be found in [5,9].

With the cohesive elements approach, a coarser mesh can be used compared to VCE. Moreover, the crack propagation is simulated in a natural way as it is related to the local loss of mechanical properties of the material assigned to the interface. For instance in pure mode loading, once the energy below the curve of Figure 6 (which is directly linked to the fracture toughness) is dissipated, damage is equal to 1 and the interface is locally broken. With LMS Samtech Samcef, defining zero-thickness interface elements in an existing mesh is a very simple task. Consequently, there is no inconvenience associated to the meshing process. Using the cohesive laws of Figure 6 requires more parameters compared to VCE. However, this is no more an issue today as the procedure to identify these parameters is available at the coupon level based on, for instance, the DCB and ENF tests as explained in [1].

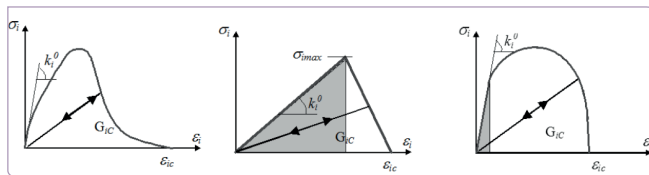


Fig. 6: Possible constitutive laws in the interface

Application

The test case is illustrated in Figure 7. It is a laminated composite element made of carbon/epoxy skin and stiffener, supported at its edges along direction 1 and submitted to a pull test. Initial delaminations (i.e. initial cracks) are defined between each ply in the middle region of the structure, on a square zone, as well as at the noodle location. Thus, 83 initial crack fronts are taken into account in the structure (Figure 7). The initial cracks are modelled by double nodes. Solid shell elements are used. The laminates are made up of plies oriented at 0° , 90° , 45° and -45° . The dimensions, stacking sequences, number of plies and base material properties are not reported here, for confidentiality reasons. Simulation is used here as a predictive tool, and the physical and virtual test results are finally compared in order to estimate the efficiency of the finite element software.

First, VCE is used to detect the most dangerous cracks in the problem. The model of Figure 8 includes 1,028,080 degrees of freedom. Refinements are defined in the vicinity of the crack fronts in order to satisfy the requirements on the mesh

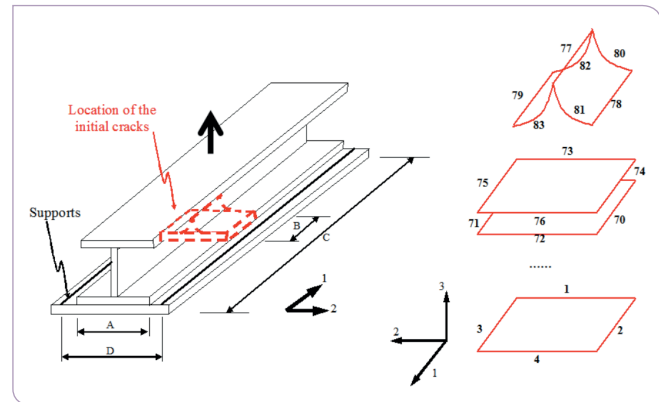


Fig. 7: Location of the cracks in the composite element submitted to a pull test

size needed to obtain accurate results [5]. It then comes that elements of an in-plane size of about 0.5mm are used in the zones of interest. Two elements are used along each ply thickness; that is, multi-layer elements are not used. A very large number of contact elements (14,186) is defined in the model (Figure 9). It is indeed essential to avoid ply penetration in order to obtain physical and accurate results. A given value of the vertical load is imposed on the upper face, via rigid body elements. A linear static analysis is conducted. The evolution of the failure criterion (1) for these initial cracks is also provided. It is clear from Figure 10 that 3D effects appear in the problem, even if a simple pull test is conducted. Indeed, not only mode I but also mode II are present in the problem and their magnitude is of the same order (mode III is not represented). The results of Figure 10 indicate that the cracks at the noodle loca-

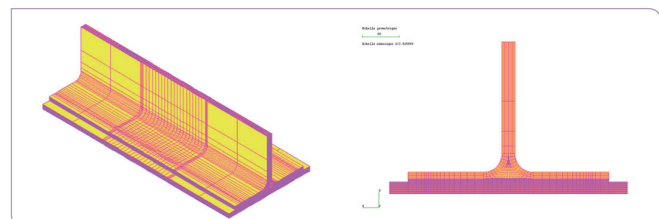


Fig. 8: Finite element model for VCE

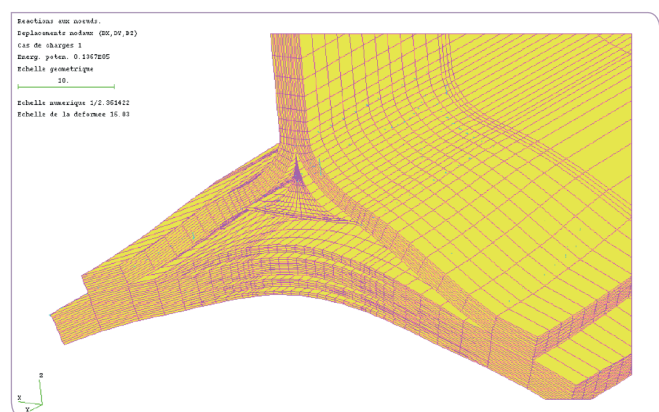


Fig. 9: Deformation of the element and ply penetration avoided thanks to contact elements

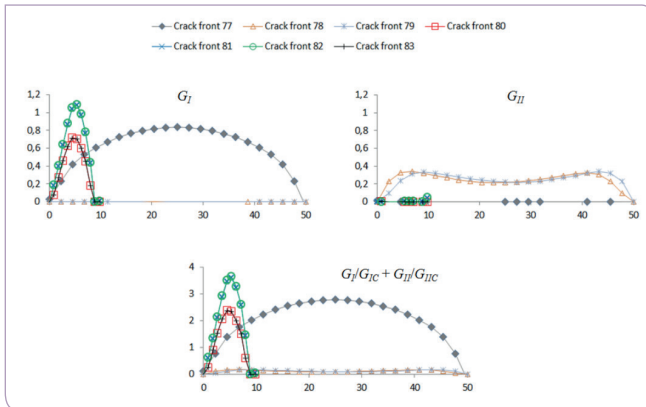


Fig. 10: Evolution of the failure criterion along the crack fronts (crack front numbering given in Figure 7)

tion (as defined in Figure 7) are the most dangerous ones. Then, the propagation of the initial cracks is studied with the cohesive elements approach. The model is illustrated in Figure 11, with the 3D cohesive elements defined in the extension of each initial crack (Figure 12). The model includes a total of 126,697 degrees of freedom, and 3,054 interface elements. The internal voids in Figure 12 correspond to the initial cracks, modelled with double nodes: interface elements are not defined at these locations but contact elements are used to avoid penetration. One element is used along each ply thickness. A vertical displacement is imposed on the upper face. A non-linear static analysis is conducted as the mechanical properties in the interfaces will evolve according to the non-linear laws of Figure 6. Here, the bi-triangular law is used. The evolution of the damage inside the interface elements is illustrated in Figures 13 and 14. It is clear that delamination is initiated at the nodal location, as previously predicted with the VCE method. However, the final collapse is due to the skin/stiffener separation. The reaction/displacement curve is plotted in Figure 15. The test result is compared to the prediction obtained by simulation: a very good agreement is obtained. The evolution of the composite element stiffness is well represented and the simulation over-estimates the maximum force by only 5%. The first crack propagation is indicated by a black circle in Figure 15, for a level of reaction force which is far from the maximum value the composite part can sustain. The computation time is 74 minutes. Even though a parallel solver is available in LMS Samtech Samcef, a single processor is used here (Bi-Xeon 5160 3GHz machine, 16 GB central memory, 64-bit RedHat AS 4 UP4).

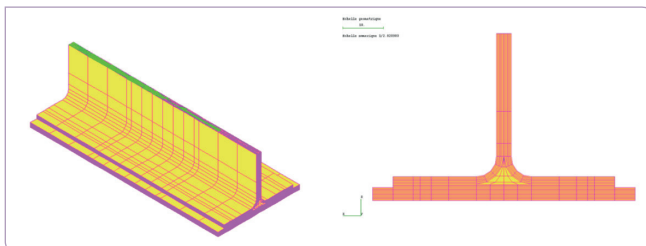


Fig. 11: Finite element model for the cohesive elements approach

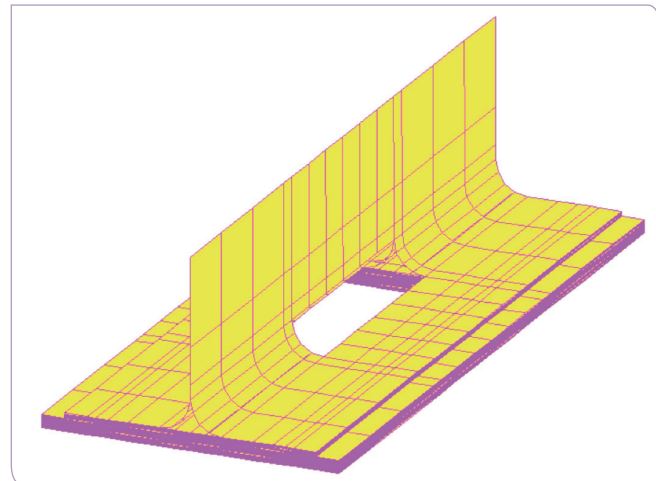


Fig. 12: Group of interface elements

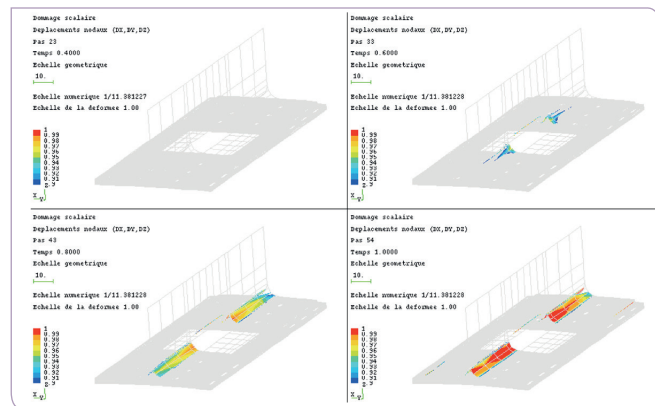


Fig. 13: Damage evolution in the interfaces for an increasing value of the imposed displacement

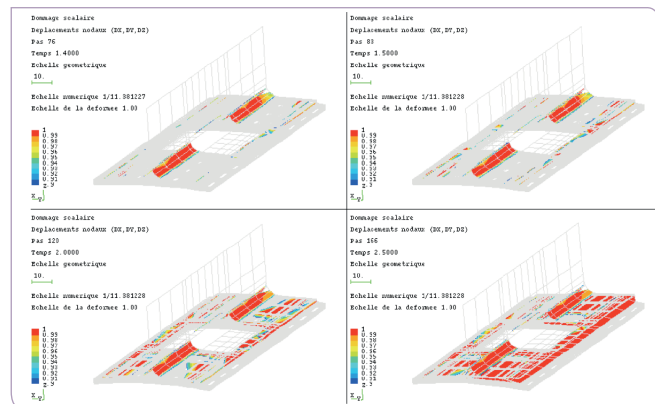


Fig. 14: Damage evolution in the interfaces for an increasing value of the imposed displacement [continued]

Conclusion

Modelling and solving delamination problems in composites are known to be difficult, and the virtual testing capabilities offered by LMS Samtech Samcef comply with the industrial reality. Some of the needs identified at the industrial level include using large-size finite element models to effi-

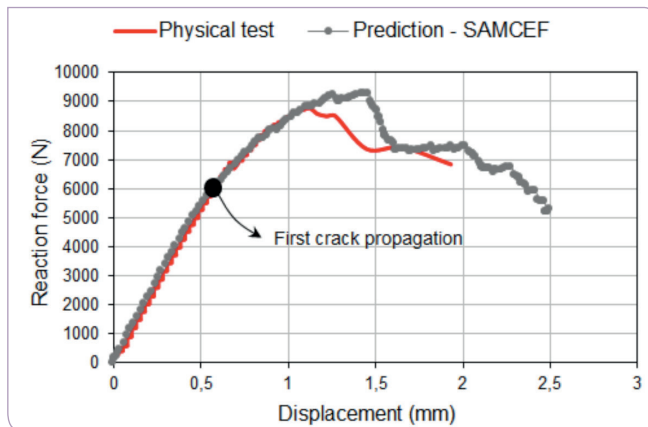


Fig. 15: Reaction/displacement curves from SAMCEF prediction and test

More information

Additional tests run on a variant of this problem (different dimensions, material, stacking sequence, boundary conditions) showed a small sensitivity of the solution to the mesh size when the cohesive element approach is used (Figure a). The LMS Samtech Samcef parallel solver can be used to decrease the computational time even more (Figure b and Table 1). Here, a speedup of 3 is obtained with 4 processors, resulting in an efficiency of 75%.

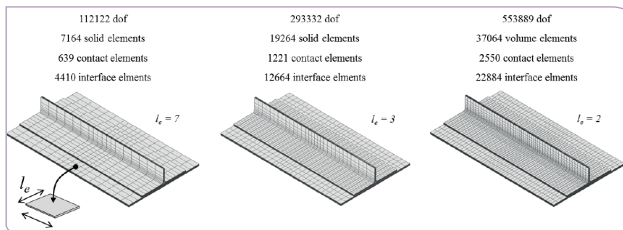


Fig. a: Different mesh refinements of the model (l_e = average in-plane element length)

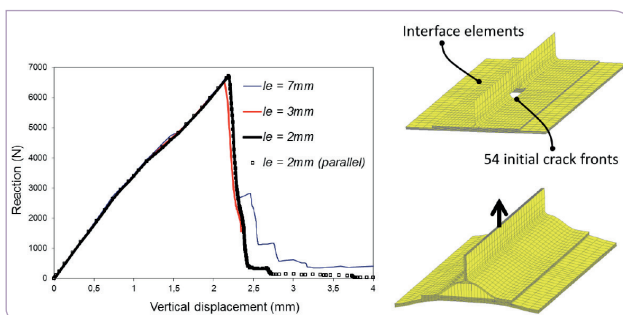


Fig. b: Load-displacement curves for different mesh refinements of the model

Computational times (in minutes) needed to solve the industrial problem

Mean l_e (mm)	Number of processors	Size of the problem dof	Maximum load (N)	CPU to reach 2.35mm (minutes)
2	4	553,889	6,700	285
2	1	553,889	6,700	854
3	1	293,332	6,530	524
7	1	112,122	6,720	44

ciently represent reality; taking a large number of cracks in the structure into consideration in order to provide a safe design; modelling contact conditions over large areas; and obtaining accurate results. LMS Samtech Samcef efficiently answers these industrial concerns with features such as easy definition of cracks and delamination zones; estimation of the propagation load via the VCE method; more advanced capabilities through the cohesive elements approach for interlaminar crack propagation and estimation of the overall structural behaviour during the fracture process; a library of softening material laws for interlaminar behaviours; efficient strategies for treating contact conditions; accurate results (compared to reference solutions); and a parallel solution procedure for large-scale problems. ■

References

- [1] Bruyneel M., Delsemme J.P., Goupil A.C., Jetteur P., Lequesne C., Naito T., Urushiyama Y. "Damage modeling of laminated composites: validation of the inter-laminar damage law of LMS Samtech Samcef at the coupon level for UD plies". 11th World Congress on Computational Mechanics (WCCM XI), July 20-25, 2014, Barcelona, Spain.
- [2] Bruyneel M., Delsemme J.P., Goupil A.C., Jetteur P., Lequesne C., Naito T., Urushiyama Y. "Damage modeling in laminated composites: validation of the intra-laminar damage law of LMS Samtech Samcef at the coupon level for UD plies". European Conference on Composite Materials (ECCM16), June 22-26, 2014, Seville, Spain.
- [3] Bruyneel M., Degenhardt R. and Delsemme J.P. "An industrial solution to simulate post-buckling and damage of composite panels". JEC Composites Magazine, 48, May 2009.
- [4] Galucio A.C., Jetteur P., Trallero D. and Charles J.P. "Toward numerical fatigue prediction of composite structures: application to helicopter rotor blades". 3rd ECCOMAS Thematic Conference on the Mechanical Response of Composites, September 2011, Hannover, Germany.
- [5] Bruyneel M., Delsemme J.P., Jetteur P., Germain F. "Modeling inter-laminar failure in composite structures: illustration on an industrial case study". Applied Composite Materials, 16(3), 149-162, 2009.
- [6] Krueger R. "An approach to assess delamination propagation simulation capabilities in commercial finite element codes". NASA/TM-2008-215123, 2008.
- [7] Krueger R., Rinderknecht S., Koning M. "Two- and Three-Dimensional Finite Element Analyses of Crack Fronts in a Multidirectional Composite ENF Specimen", ISD-Report No. 97/1, University of Stuttgart, 1997.
- [8] Orifici, A. R. S., Thomson, Degenhardt R., Bisagni C., Bayandor J. "An analysis tool for design and certification of post-buckling composite aerospace structures". International Journal of Structural Stability and Dynamics, 10, pp. 669-683, 2010.
- [9] Allix O. and Ladevêze P. "Interlaminar interface modeling for the prediction of laminate delamination", Composite Structures, 22, 235-242, 1992.
- [10] Jetteur, Ph., "Modèle Matériau pour l'Elément d'Interface", SAMTECH Report RS-246, 2006.